

Dual-Gate AlGaIn/GaN Modulation-Doped Field-Effect Transistors with Cut-Off Frequencies $f_T > 60$ GHz

Ching-Hui Chen, Robert Coffie, K. Krishnamurthy, Stacia Keller, Mark Rodwell, *Member, IEEE*, and Umesh K. Mishra, *Fellow, IEEE*

Abstract—We demonstrate dual-gate AlGaIn/GaN modulation-doped field-effect transistors (MODFETs) with gate-lengths of 0.16 μm and 0.35 μm for the first and second gates, respectively. The dual-gate device exhibits a current-gain cut-off frequency $f_T > 60$ GHz, and can simultaneously achieve a high breakdown voltage of $>+100$ V. In comparison to single-gate devices with the same gate length 0.16 μm , dual-gate FETs can significantly increase breakdown voltages, largely increasing the maximum allowable drain bias for high power application. The continuous wave (CW) output power is in excess of 3.5 W/mm at 8.2 GHz. The corresponding large-signal gain is 12 dB and the power added efficiency is 45%. The dual-gate device with different gate lengths shows the capability of providing simultaneous high cut-off frequencies, and high breakdown voltages for broadband power amplifiers.

Index Terms—AlGaIn/GaN, broadband power amplifiers, dual-gate FETs.

I. INTRODUCTION

THE 2–20 GHz PHASED array radars, now in development, require amplifiers operating over a decade bandwidth while providing tens to hundreds of watts with high power added efficiency. GaN/AlGaIn-based devices exhibit large breakdown voltages (V_{br}) that enable the use of higher drain biases than typically used in other material systems to generate larger amounts of power ($P_{out} \leq V_{br}^2/8R_L$) for high power electronics. Extensive efforts toward improving microwave performance of AlGaIn/GaN modulation-doped field-effect transistors MODFETs have been made in the past years [1]–[3], focusing on extending output power and cutoff frequencies, f_T . An output power density of 9.1 W/mm at 8.2 GHz has been demonstrated on SiC substrate [4] and a higher $f_T > 110$ GHz has also been achieved with a gate-length $L_g < 0.1 \mu\text{m}$ [5].

In broadband common-source power amplifiers, the gain bandwidth product is limited to approximately f_T . Increased f_T can be obtained by reducing the gate length L_g , however, the breakdown voltage V_{br} will be significantly reduced.

Manuscript received February 10, 2000; revised June 2, 2000. This work was supported by the Office of Naval Research through a grant monitored by Dr. J. Zolper, Contract N0014-98-1-0750 at the University of California, Santa Barbara, and by a National Science Foundation Graduate Fellowship. The review of this letter was arranged by Editor D. Ueda.

The authors are with the Department of Electrical and Computer Engineering, University of California, Santa Barbara, CA 93106 USA (e-mail: rcoffie@indy.ece.ucsb.edu).

Publisher Item Identifier S 0741-3106(00)10827-4.

In the Johnson limit [6], the product of $V_{br}f_T$ is less than $E_{max}v_{sat}/\pi$, where E_{max} and v_{sat} are the breakdown field and the electron velocity. Increased V_{br} is obtained at the expense of decreased f_T , and high power levels are obtained at the expense of reduced amplifier bandwidth.

AlGaIn/GaN dual-gate devices have the potential of simultaneously realizing a high f_T and a high breakdown voltage. Moreover, smaller feedback capacitance and higher output impedance of dual-gate devices enable flexibility for circuit application of broadband power amplifiers. A dual-gate device is electrically equivalent to a common-source (CS)/common-gate (CG) cascode pair, but occupies less die area. The current gain of the dual-gate device, $h_{21}(jf) = (f_{T1}/jf)(1 + jf/f_{T2})^{-1}$, deviates from that of the CS device $h_{21}(jf) = (f_{T1}/jf)$, only for $f > f_{T2}$, where f_{T1} and f_{T2} are the current gain cutoff frequencies of the CS and CG devices and f is the signal frequency. To provide substantial current gain, f_{T1} must be several times of the signal frequency f . In contrast, to avoid significant loss (i.e., $>10\%$) in h_{21} in the CG stage, it is sufficient to have f_{T2} of 1.5 f to 2 f . The breakdown voltage is however determined by the CG device. Therefore, in a dual-gate device, it is advantageous to design the CS device with short L_g hence high f_T , and the CG device with long L_g hence lower f_T , but improved V_{br} . High bandwidth and high power are thus simultaneously obtained. In this paper, we report AlGaIn/GaN dual-gate MODFETs with gate lengths of 0.16 μm and 0.35 μm for the first and second gate, respectively. A high $f_T > 60$ GHz and a high breakdown voltage of $>+100$ V can be simultaneously achieved for AlGaIn/GaN MODFETs.

II. DEVICE FABRICATION

The epilayers of Al_{0.3}Ga_{0.7}N/GaN dual-gate devices were grown by metal organic chemical vapor deposition (MOCVD) on a c-plane sapphire substrate. The material structure began with a 200 Å thick GaN nucleation layer, followed by 3 μm thick insulating i-GaN as a device buffer layer. The Al_{0.3}Ga_{0.7}N contains a 30 Å unintentionally doped spacer layer, a 120 Å Si-doped charge supply layer and a 50 Å thick cap layer. Sheet electron concentration and electron Hall mobility of as-grown wafer were $\sim 1.02 \times 10^{13} \text{ cm}^{-2}$ and 1400 $\text{cm}^2/\text{V}\cdot\text{s}$ at room temperature.

Ti/Al/Ni/Au (200 Å/2000 Å/550 Å/450 Å) ohmic contacts were evaporated and then annealed at 880 °C for 30 s. Gate

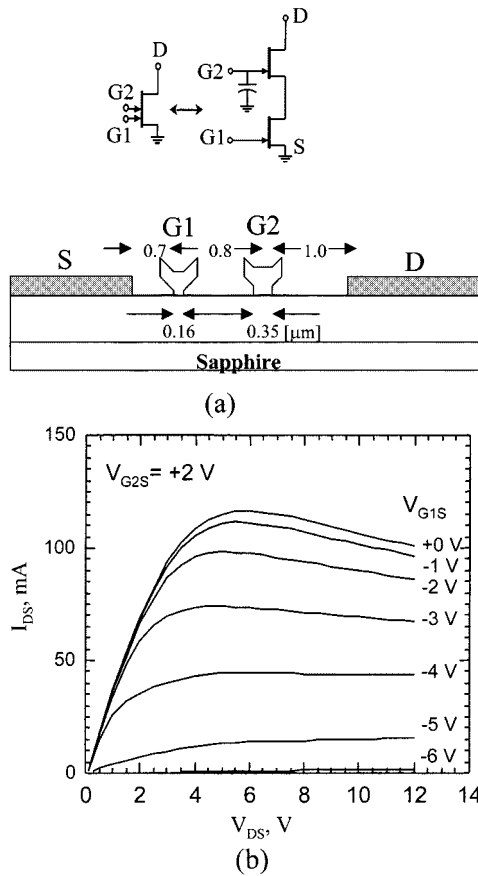


Fig. 1. (a) Schematic diagram of GaN/AlGaN dual-gate FETs (b) Drain output I - V characteristics of $0.16/0.35 \times 150 \mu\text{m}$ dual-gate MODFET's with second gate biased at +2 V.

lithography was performed with a JEOL JBX-5DII (U) electron beam system. Both T-shaped gates with 0.16 and $0.35 \mu\text{m}$ footprints separated by $0.8 \mu\text{m}$ were produced with a PMMA/P(MMA-MAA)/PMMA tri-layer resist to reduce the resistance of submicrometer gates. Ni/Au/Ni ($200 \text{ \AA}/3700 \text{ \AA}/300 \text{ \AA}$) were then evaporated as gate metals. The gate of CG device was connected to the source of the CS device using MIM capacitors with 1600 \AA SiO_2 , providing RF grounding, and then a thick Ni/Au layer ($\sim 4500 \text{ \AA}$) was evaporated on the top of the SiO_2 capacitors as the second gate pads. The final step in the process was to form a device mesa with Cl_2 reactive ion beam etching. The first gate was separated by $0.7 \mu\text{m}$ from the source, and the second gate was $1 \mu\text{m}$ away from the drain contact. A schematic diagram of the finished dual-gate device is shown in Fig. 1(a).

III. DEVICE CHARACTERISTICS AND DISCUSSION

The common source dc characteristics of the dual-gate device with the second gate biased at +2 V are shown in Fig. 1(b). The saturation current, I_{DSS} , is about 0.8 A/mm and pinch-off voltage is -6 V . The peak value of extrinsic transconductance, g_m , is about 220 mS/mm at V_{G2S} of +2 V. The average values of contact resistance and sheet resistance are $0.9 \Omega\text{-mm}$ and $500 \Omega/\square$, respectively. As seen in Fig. 2, the breakdown voltages of $0.16 \mu\text{m}$ single-gate FETs were less than +50 V, which is typical of such short-channel GaN/AlGaN MODFETs [8]. The

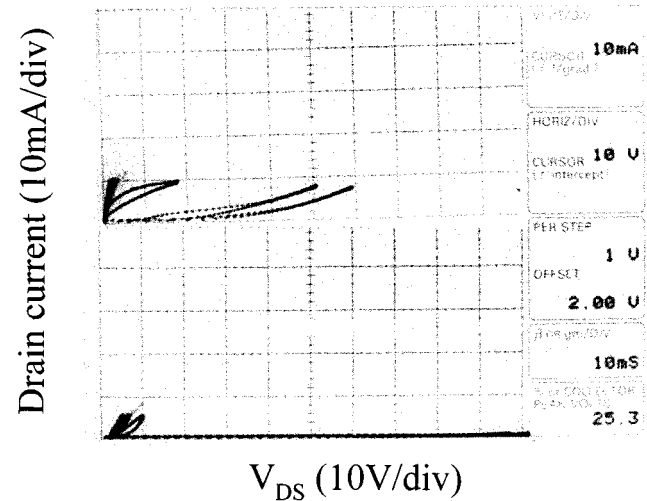


Fig. 2. Comparison of breakdown behaviors of single-gate and dual-gate GaN/AlGaN MODFETs fabricated on the same wafer. The dual-gate device increases three-terminal breakdown voltage up to +100 V.

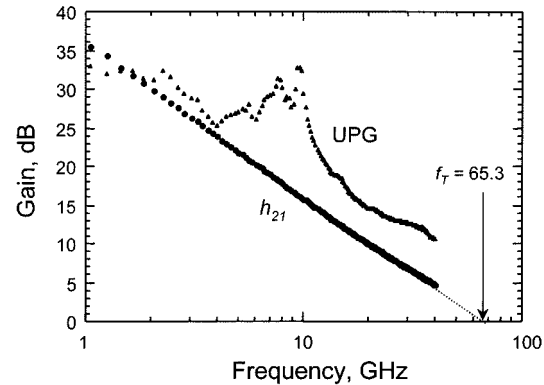


Fig. 3. Comparison of RF performance between single and dual gate devices fabricated on the same wafer: (a) S_{11} , (b) S_{22} , (c) S_{12} , and (d) S_{21} . The single-gate device was biased at $V_{DS} = +12 \text{ V}$ and $V_{GS} = -3 \text{ V}$, and the dual-gate device was operated with bias voltages of $V_{G2S} = +2 \text{ V}$, $V_{DS} = +12 \text{ V}$ and $V_{G1S} = -3 \text{ V}$.

$0.16/0.35 \mu\text{m}$ dual-gate FETs had larger breakdown voltages of over +100 V. The reason for the increased breakdown voltage is the drain voltage is supported by the longer gate, which has a higher breakdown voltage because of electric field alleviation as discussed in [7]. Since the drain voltage swing of CS device is limited to the pinch-off voltage of CG device, leakage associated with large drain voltage excursions in short-channel devices is eliminated. Therefore, the maximum allowable drain bias is increased for high frequency and high power amplifiers.

DC to 40 GHz device S-parameters were measured at a V_{DS} of +13.5 V, I_{DS} of 240 mA/mm , and a V_{G2S} of +2 V. Both CS and CG devices, we biased in the saturation region. Fig. 3 shows the h_{21} and unilateral power gain (UPG) of dual-gate devices. The dual-gate device exhibits $f_T > 65 \text{ GHz}$ and $f_{max} > 100 \text{ GHz}$. Since the current gain of dual-gate devices follows $h_{21}(jf) = (f_{T1}/jf)(1+jf/f_{T2})^{-1}$, h_{21} of the dual-gate FETs is within roughly 10 to 20% of that of the single-gate device at the frequencies measured. Fig. 4 shows a comparison of RF performance between single-gate and dual-gate devices. Due to the presence of the second gate, the dual-gate device substantially

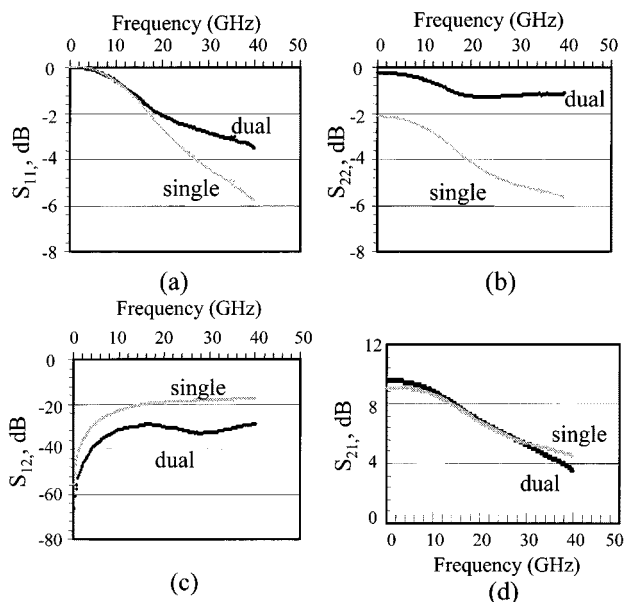


Fig. 4. Gain-frequency characteristics of dual-gate AlGaIn/GaN MODFETs.

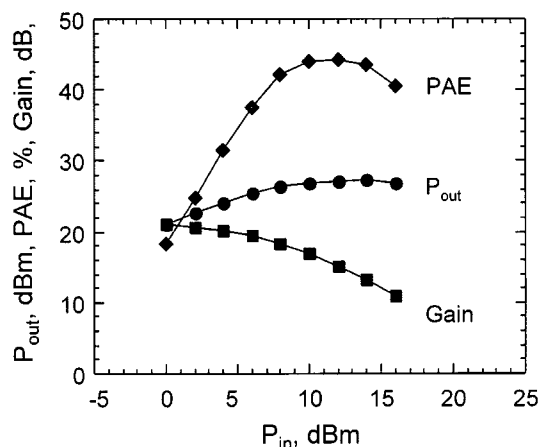


Fig. 5. Microwave power performance of dual-gate device at 8.2 GHz, with bias voltages of $V_{GS} = +2$ V and $V_{DS} = +20$ V. The output power is greater than 3.5 W/mm, and the small signal gain, PAE, and large signal gain are 21.5 dB, 45% and 12 dB, respectively.

reduces signal feedback (S_{12}) more than 10 dB and increases output impedance (S_{22}) by 4 dB, leading to increased device power gain [9], [10]. It was noted that the maximum stable gain (MSG) and maximum available gain (MAG) of dual-gate devices were increased by 6 dB below 17 GHz, in comparison with single-gate devices. RF continuous wave (CW) power measurements were performed on uncooled devices on a sapphire

substrate at 8.2 GHz. Fig. 5 shows the power performance of dual-gate devices biased at a V_{DS} of +20 V, with the second gate bias voltage of +2 V. The drain current at peak output power was 48 mA (320 mA/mm). The output power density is higher than 3.5 W/mm. The small-signal gain, power-added efficiency (PAE), and large-signal gain are 21.5 dB, 45% and 12 dB, respectively. Unfortunately, the higher breakdown voltage afforded by this scheme could not be effectively utilized because of substrate heating effects beyond a bias of +25 V.

IV. CONCLUSIONS

In conclusion, we have demonstrated dual-gate AlGaIn/GaN MODFETs with T-shaped gates of 0.16 and 0.35 μm footprints on a c-plane sapphire substrate. A CW output power in excess of 3.5 W/mm was achieved at 8.2 GHz, with power-added efficiency >45%. The dual-gate device shows a capability of providing the desired characteristics of a high f_T (>60 GHz), while still maintaining a large breakdown (>+100 V) for broadband power amplifiers.

ACKNOWLEDGMENT

The authors are grateful to Dr. Y. Wu at Nitres, Inc. for several useful discussions.

REFERENCES

- [1] Y.-F. Wu *et al.*, "GaIn-based FET's for microwave power amplification," *IEICE Trans. Electron.*, vol. E82-C, pp. 1895–905, 1999.
- [2] A. T. Ping *et al.*, "DC and microwave performance of high-current AlGaIn/GaN heterostructure field effect transistors grown on p-type SiC substrates," *IEEE Electron Device Lett.*, vol. 19, pp. 54–56, 1998.
- [3] S. T. Sheppard *et al.*, "High-power microwave GaIn/AlGaIn HEMT's on semi-insulating silicon carbide substrate," *IEEE Electron. Device Lett.*, vol. 20, pp. 161–163, 1999.
- [4] Y. F. Wu *et al.*, "High Al-content AlGaIn/GaN HEMT's on SiC substrates with very-high power performance," in *IEDM Tech. Dig.*, 1999, IEDM 99–925.
- [5] N. X. Nguyen, "Private communication," unpublished, 1999.
- [6] E. O. Johnson, "Physical limitations on frequency and power parameters of transistors," *RCA Rev.*, pp. 163–177, 1965.
- [7] T. M. Barton and P. H. Ladbrooke, "The role of the device surface in the high voltage behavior of the GaAs MESFET," *Solid-State Electron.*, vol. 29, pp. 807–813, 1986.
- [8] K. K. Chu, J. A. Smart, J. R. Shealy, and L. F. Eastman, "AlGaIn-GaN piezoelectric HEMT's with submicron gates on sapphire," in *Proc. Conf. Compound Semiconductor Power Transistors and State-of-the-Art Program on Compound Semiconductors (SOTAPOCS XXIX)*, Boston, MA, Nov. 1998.
- [9] S. Asai, F. Murai, and H. Kodera, "GaAs dual-gate Schottky-barrier FET's for microwave frequencies," *IEEE Trans. Electron Devices*, vol. ED-22, pp. 897–904, Oct. 1975.
- [10] Y. K. Chen, G. W. Wang, D. C. Radulescu, and L. F. Eastman, "Comparison of microwave performance between single-gate and dual-gate MODFETs," *IEEE Electron. Device Lett.*, vol. 9, pp. 59–61, Feb. 1988.